Published in "Molecular & Cellular Proteomics doi: 10.1074/mcp.RA117.000437, 2018" which should be cited to refer to this work.

Combinatorial omics analysis reveals perturbed lysosomal homeostasis in collagen VII-deficient keratinocytes

Kerstin Thriene[1,2], Björn Andreas Grüning[2,3], Olivier Bornert[1], Anika Erxleben[2,3], Juna Leppert[1], Ioannis Athanasiou[1], Ekkehard Weber[4], Dimitra Kiritsi[1], Alexander Nyström[1], Thomas Reinheckel[5,6], Rolf Backofen[2,3,6], Cristina Has[1], Leena Bruckner-Tuderman[1,2,6,*], Jörn Dengjel[1,2,6,7,*]

[1]Department of Dermatology, Medical Center - University of Freiburg, Germany

[2]Centre for Biological Systems Analysis (ZBSA), University of Freiburg, Germany

[3]Department of Computer Science, University of Freiburg, Germany

[4]Institute of Physiological Chemistry, Medical Faculty, Martin Luther University Halle-Wittenberg, Germany

[5]Institute of Molecular Medicine and Cell Research, Faculty of Medicine, University of Freiburg, Germany

[6]Centre for Biological Signalling Studies (BIOSS), University of Freiburg, Germany

[7]Department of Biology, University of Fribourg, Switzerland

Running title: perturbed homeostasis in C7-deficient keratinocytes

* Corresponding authors:

Jörn Dengjel (Lead Contact), Dep. of Biology, University of Fribourg, Chemin du Musée 10, 1700 Fribourg, Switzerland; email: joern.dengjel@unifr.ch; phone: +41 26 300 8631; fax: +41 26 300 9741

Leena Bruckner-Tuderman, Dep. of Dermatology, Medical Center - University of Freiburg, Hauptstr. 7, 79104 Freibrug, Germany; email: bruckner-tuderman@uniklinik-freiburg.de ; phone: +49-761-270-67160; fax: +49-761-270-69360

Abbreviations

BH: Benjamini-Hochberg

BM: basement membrane

C7: collagen VII

CAF: cancer-associated fibroblasts

ECM: extracellular matrix

DEJZ : dermal-epidermal junction zone

DEB: dystrophic epidermolysis bullosa

MS: mass spectrometry

NHK: normal human keratinocytes

PCA: principal component analysis

SCC: squamous cell carcinoma

SILAC : stable isotope labelling by amino acids in cell culture

SOTA: self-organizing tree algorithm

Summary

The extracellular matrix protein collagen VII is part of the microenvironment of stratified epithelia and critical in organismal homeostasis. Mutations in the encoding gene *COL7A1* lead to the skin disorder dystrophic epidermolysis bullosa (DEB), are linked to skin fragility and progressive inflammation-driven fibrosis that facilitates aggressive skin cancer. So far, these changes have been linked to mesenchymal alterations, the epithelial consequences of collagen VII loss remaining under-addressed. As epithelial dysfunction is a principal initiator of fibrosis, we performed a comprehensive transcriptome and proteome profiling of primary human keratinocytes to generate global and detailed images of dysregulated epidermal molecular pathways linked to loss of collagen VII. These revealed downregulation of interaction partners of collagen VII on mRNA and protein level, but also increased abundance of S100 pro-inflammatory proteins in primary DEB keratinocytes. Increased TGF-β signaling due to loss of collagen VII was associated with enhanced activity of lysosomal proteases in both keratinocytes and skin of collagen VII-deficient individuals. Thus, loss of a single structural protein, collagen VII, has extra- and intracellular consequences, resulting in inflammatory processes that enable tissue destabilization and promote keratinocyte-driven, progressive fibrosis.

Keywords: inflammation, fibrosis, keratinocyte, mass spectrometry, collagen, proteases, lysosome, autophagy, TGF-β, extracellular matrix, dystrophic epidermolysis bullosa (DEB)

Introduction

The cellular microenvironment encompasses structural components, the extracellular matrix (ECM), and soluble factors, e.g. growth factors (1). The ECM was initially regarded as purely structural scaffold keeping cells in place and ensuring tissue/organ integrity. Through the discovery of ECM-cell contact sites and underlying signaling events, the crucial role of the ECM for cell survival, proliferation and differentiation emerged (1,2). Importantly, it is now clear that a dysregulated ECM can actively promote disease progression in humans (3). The skin contains a particular complex ECM, the dermal-epidermal junction zone (DEJZ), which binds the epidermis and the dermis and is generated by cell types of distinct epithelial and mesenchymal linages: keratinocytes, the main cell type of the epidermis, and fibroblasts, the main mesenchymal-derived cell type of the dermis. The DEJZ is vital for skin integrity. As part of the DEJZ the ECM protein collagen VII (C7) forms anchoring fibrils, which entrap dermal fibrils and establish stable dermal-epidermal adhesion (4).

Biallelic loss-of-function mutations of the gene *COL7A1* encoding C7 cause dystrophic epidermolysis bullosa (DEB), an inherited skin fragility disorder characterized by a broad spectrum of clinical manifestations: skin blistering, abnormal wound healing, excessive scarring often resulting in aggressive skin cancer (5). However, the variety and multitude of the symptoms are not easily explained by the underlying *COL7A1* mutations.

Toward this end ‘omics’ approaches have been used to delineate the cellular and microenvironmental consequences of C7 loss. However so far, mainly the consequences of C7-deficiency on already transformed squamous cell carcinoma cells (6,7), and on dermal fibroblasts were addressed (8,9). Transcriptome analyses have suggested that the gene expression profile of DEB fibroblasts resembles that of cancer-associated fibroblasts (CAFs) and that loss of C7 may generate a permissive microenvironment for tumor development (9). Quantitative mass spectrometry (MS)-based proteomics studies using DEB fibroblasts focused on the extracellular consequences of the absence of C7 and revealed reduction of basement membrane proteins and increase of dermal matrix proteins, highlighting the multifaceted roles of C7 (8). Reduced crosslinking of dermal ECM proteins due to lower abundance of

4

transglutaminase 2, an interaction partner of C7, indicated altered mechanical properties of the fibroblast microenvironment due to loss of C7 (10).

It has become apparent that progressive TGF-β-mediated soft tissue fibrosis plays a major role in disease evolution of DEB (11,12). In other diseases epithelial dysfunction is known to be a major instigator of fibrosis (13). Known for DEB is that C7 as a master regulator of laminin-332 deposition may exert control over the laminin-332-integrin α6β4 signaling axis (Nystrom et al., 2013). However, the potential contribution of these and additional epithelial alterations to progression of DEB remain elusive. Therefore, we performed a global transcriptome and proteome profiling comparing primary DEB keratinocytes to normal human keratinocytes (NHK), delineating C7-dependent molecular pathways dysregulated in disease. We combined high-throughput sequencing using RNAseq with stable isotope labeling by amino acids in cell culture (SILAC)-based quantitative MS followed by bioinformatics analyses to address alterations in primary human keratinocytes and in skin of affected individuals. Loss of C7 did not only affect the composition of the cellular microenvironment, but it led to global changes in cell homeostasis on mRNA and on protein level. Altered abundance of ECM proteins and integrin receptors indicated dysregulated TGF-β activity caused by disruption of laminin-332-integrin α6β4 signaling. Indeed, TGF-β-dependent inflammatory and proteolytic processes were perturbed both in keratinocytes *in vitro* and in human DEB skin *in vivo*. Thus, we provide a detailed image of dysregulated molecular pathways in genetic skin fragility and show that loss of C7 leads to far more complex changes as anticipated. Importantly, our study reveals intrinsic epidermal alterations directly caused by C7 deficiency and increased TGF-β signaling in epidermal keratinocytes as instigators of dermal fibrosis.

Experimental Procedures

More information about procedures can be found online in the Supplemental Information.

Patients and DEB diagnosis

Skin specimens were obtained from ten DEB patients (DEB1-10) for diagnostic purposes and the remaining material was used for research purposes after informed consent of the patients and approval of the Ethics Committee of the University of Freiburg. The study was conducted according to the Declaration of Helsinki. Specimens are stored in an internal collection. Immunofluorescence mapping revealed lack of C7 in the skin of all patients. Mutation analysis of the C7 gene, *COL7A1* was performed as described before and disclosed mutations that lead to premature stop codons, thus confirming the diagnosis of severe generalized DEB (Table 1) (14,15). In order to elucidate disease mechanisms DEB keratinocytes were compared to primary human keratinocytes (Ctrl1-12) derived from age-matched healthy donors (Table 2). Cells used for each experiment are indicated in the respective figure according to the designations introduced in Tables 1 and 2.

Patient DEB9 had a severe generalized DEB with lack of C7 in the affected skin, as shown in a skin biopsy taken from scarred, not acutely blistered or inflamed skin next to the left knee (Supplemental Figure S6). A skin biopsy taken from a clinically unaffected skin patch on the left knee revealed C7 re-expression at around 70% of the biopsy's width. A subsequent analysis of the *COL7A1* gene from keratinocytes of the unaffected skin patch confirmed the correction of the *COL7A1* gene on one allele (data not shown).

Experimental Design and Statistical Rationale

In total, we analyzed 22 primary cell populations as listed in tables 1 and 2. `Omics` analyses were performed from two primary DEB and normal human keratinocyte populations, each. As DEB is a rare disease (less than 10 of one million newborns are affected), not more primary cells could be used for `omics` analyses. For SILAC-based proteomics analyses two biological replicates each were analyzed using swapped labels.

6

All statistical tests were corrected for multiple testing as outlined in the respective paragraphs.

Cell lysates and ECM isolation of keratinocytes for MS analysis

A SILAC approach was used to compare DEB keratinocytes to normal controls by MS-based proteomics. $5x10^5$ fully SILAC-labeled keratinocytes were seeded on 10 cm^2 cell culture dishes. On the following day, the medium was exchanged and 50 µg/mL ascorbate was added to allow proper maturation and secretion of collagens (16). Keratinocytes were kept in culture for six days and fresh culture medium containing ascorbate was added daily. After six days, keratinocytes were washed 3 times with DPBS. The cells were removed from the underlying ECM through incubation with 0.5% Triton X-100 in DPBS for 10 s, followed by a washing step with DPBS and an incubation for 10 s with 20 mM NH_4OH in DPBS (17). Cell lysates were concentrated by ultrafiltration using vivaspin columns (10 kDa MWCO). The remaining ECM was carefully washed 3 times with DPBS to eliminate intracellular contaminants and then solubilized with 4% SDS in 0.1 M Tris–HCl, pH 7.6 (18). Aliquots of the different ECM samples or cell lysates were used for WB analysis or mixed 1:1:1 and prepared for MS analysis in order to test accurate mixing ratios. Mixing was adjusted for actual MS analysis afterwards.

MS sample preparation

In-gel digestion. Samples were heated in SDS-PAGE loading buffer, reduced with 1 mM DTT for 5 min at 95°C and alkylated using 5.5 mM iodoacetamide for 30 min at room temperature. Protein mixtures were separated on 4-12% gradient gels. The gel lanes were cut into 10 equal slices, the proteins were in-gel digested with trypsin and the resulting peptide mixtures were processed on STAGE tips and analyzed by LC-MS/MS (19,20).

Mass Spectrometry

MS measurements were performed on an LTQ Orbitrap XL mass spectrometer coupled to an Agilent 1200 nanoflow–HPLC. HPLC–column tips (fused silica) with 75 µm inner diameter were self-packed with Reprosil–Pur 120 ODS–3 to a length of 20 cm. Samples were applied directly

7

onto the column without a pre–column. A gradient of A (0.5% acetic acid in water) and B (0.5% acetic acid in 80% acetonitrile in water) with increasing organic proportion was used for peptide separation (loading of sample with 2% B; separation ramp: from 10–30% B within 80 min). The flow rate was 250 nL/min and for sample application 500 nL/min. The mass spectrometer was operated in the data–dependent mode and switched automatically between MS (max. of $1x10^6$ ions) and MS/MS. Each MS scan was followed by a maximum of five MS/MS scans in the linear ion trap using normalized collision energy of 35% and a target value of 5000. Parent ions with a charge state from z = 1 and unassigned charge states were excluded for fragmentation. The mass range for MS was m/z = 370–2000. The resolution was set to 60,000. MS parameters were as follows: spray voltage 2.3 kV; no sheath and auxiliary gas flow; ion–transfer tube temperature 125°C.

Identification of proteins and protein ratio assignment using MaxQuant

The MS raw data files were uploaded into the MaxQuant software version 1.4.1.2 for peak detection, generation of peak lists of mass error corrected peptides, and for database searches (21). A full-length UniProt human database additionally containing common contaminants such as keratins and enzymes used for in–gel digestion (based on UniProt human FASTA version September 2013, 87000 entries) was used as reference. Carbamidomethylcysteine was set as fixed modification and protein amino–terminal acetylation and oxidation of methionine were set as variable modifications. Triple SILAC was chosen as quantitation mode. Three missed cleavages were allowed, enzyme specificity was trypsin/P, mass tolerance for first search was 20 ppm, and the MS/MS tolerance was set to 0.5 Da. The average mass precision of identified peptides was in general less than 1 ppm after recalibration. Peptide lists were further used by MaxQuant to identify and relatively quantify proteins using the following parameters: peptide and protein false discovery rates, based on a forward-reverse database, were set to 0.01, minimum peptide length was set to 6, minimum number of peptides for identification and quantitation of proteins was set to one which must be unique, minimum ratio count was set to two, and identified proteins were requantified. The ‘match-between-run’ option (2 min) was

8

used. Annotated spectra of single peptide-based protein IDs are provided as Supplemental Files S1 and S2.

The mass spectrometry proteomics data have been deposited to the ProteomeXchange Consortium via the PRIDE partner repository with the dataset identifier PXD005873 (22). Reviewer account details: Username: reviewer53943@ebi.ac.uk; Password: mQMzJQFw.

9

Results

Disease-relevant transcriptional changes in primary human DEB keratinocytes

DEB keratinocytes are characterized by a loss of C7 (Figure 1A) and skin of affected individuals exhibits mechanical fragility, inflammation, excessive scarring and fibrosis (Figure 1B). Whereas disease contributions of mesenchyme-derived cells have been extensively studied, the influence of epithelial cells remains obscure, which led us to investigate the epidermal responses to loss of C7 (see Tables 1-2 and Experimental Procedures for designation of used primary cells).

To study the effects of C7 loss on the transcriptome, DEB keratinocytes from two donors and two age-matched controls were cultured to the same number of passages and the extracted RNAs were subjected to next-generation RNA sequencing. In total, expression of 39,293 gene variants was detected (Supplemental Table S1) of which 300 were differentially regulated in DEB and control keratinocytes (BH-corrected q-value 0.1) (Supplemental Table S2). To illustrate altered gene expression in DEB keratinocytes, we performed a cluster analysis of the differentially expressed genes and observed a greater variability between the two DEB cells than between the control cells (Figure 2A).

GO term analysis of differentially expressed genes revealed enrichment of GO terms like cell migration and ECM organization which are processes known to be affected by the loss of C7 (8,10) (Figure 2B). Expression of genes encoding laminin-332 (*LAMA3*/*LAMB3*/*LAMC2*) and integrin α6β4 (*ITGA6*/*ITGB4*), direct and indirect binding partners of C7, respectively, were downregulated in DEB keratinocytes. In contrast, the transcript encoding latent-transforming growth factor beta-binding protein 1 (*LTBP1*) was more abundant, indicating increased TGF-β secretion (23) and activation of a wound response program in cells devoid of C7 (Figure 2C). Taken together, next-generation RNA sequencing revealed distinct changes of mRNA levels highlighting a perturbed transcriptional regulation as a consequence of loss of C7 in primary keratinocytes. Expression of genes encoding direct and indirect binding partners of C7 were

10

found to be downregulated, while expression of genes encoding for proteins involved in response to injury and TGF-β signaling were upregulated in DEB keratinocytes.

Altered ECM proteome composition due to loss of C7

To complement transcriptome analyses and directly assess the extracellular consequences of loss of C7, we performed quantitative proteome analyses of the keratinocyte ECM using MS. Cells were cultured in the presence of ascorbate to ensure correct posttranslational modification and stable triple-helix formation of collagens. After six days, cells were removed carefully from culture dishes using Triton/PBS followed by NH_4OH/PBS (Figure 3A) (17). Remaining insoluble proteins on the culture plate were harvested with 4% SDS and were defined as ECM. Efficiency of the protocol and purity of the ECM isolation were tested by western blot (Figure 3B). Intracellular proteins corresponding to the cell compartments nucleus (TBP), Golgi apparatus (GOLGA1), endoplasmic reticulum (HSPA5) and cytosol (GAPDH) were only detected in cell lysates. ECM proteins such as the transmembrane protein collagen XVII (COL17A1) and C7, both components of the DEJZ, fibronectin (FN1) and tenascin C (TNC) were found in both, cell lysate and ECM. Thus, intracellular proteins were depleted and extracellular components were enriched in the ECM fraction.

The same primary keratinocytes as used for gene expression analyses were SILAC labeled to assess the effect of C7 deficiency on the abundances of extracellular proteins. A Super-SILAC mix of light isotope-labeled keratinocyte ECM derived from all four donors was generated and spiked into differentially heavy isotope-labeled ECM of control and DEB keratinocytes (Figure 3C) (24). Samples were fractionated by SDS–PAGE and proteins in-gel digested with trypsin (19). Generated peptides were identified and quantified by reverse-phase LC-MS/MS. 1,386 proteins were identified in two biological replicates each, of which 1,237 could be quantified in at least one sample (average correlation coefficient = 0.66; Supplemental Figure S1 and Supplemental Table S3; see Supplemental File S1 for annotated spectra of single peptide IDs). Due to the high sensitivity of modern mass spectrometers, even small amounts of contaminating intracellular proteins are detected in the ECM fraction. To distinguish them and

11

to obtain a comprehensive list of potential true ECM proteins, the original protein list was filtered: proteins defined in the "matrisome" and those annotated by the GO terms "extracellular" and/or "cell adhesion" were defined as the "ECM proteome" (25). This led to a list of 209 identified ECM proteins of which 199 were quantified in minimally one sample (Supplemental Table S4).

DEB and control ECMs were clearly distinguished by a principal component analysis (PCA) with DEB ECM being more heterogeneous than control ECM (Supplemental Figure S2). Thus, loss of C7 has global effects on the composition of keratinocyte-derived ECM. To identify groups of co-regulated proteins, proteins were clustered by a self-organizing tree algorithm (SOTA), the dataset separating into seven clusters (Figure 3D). Proteins in each cluster were tested for enriched GO terms using the program DAVID (complete list in Supplemental Table S5) (26). Cluster 1 contained proteins that were consistently downregulated in ECM of DEB keratinocytes and that are involved in basement membrane organization, cell-cell and cell-matrix adhesion. In contrast, cluster 6 comprised proteins that showed a higher abundance in DEB ECM; they are related to inflammatory processes and wound healing. For the other clusters, especially clusters 3, 4 and 5 it was clearly evident that ECM derived from DEB keratinocytes showed patient-specific effects and was more heterogeneous than control ECM. Analysis of significantly regulated ECM proteins between DEB and control ECM revealed a network of 36 proteins with known interactions (Figure 3E; Welch's t-test, Permutation-based FDR 0.05). Similar to the results obtained by transcriptome analysis, the direct and indirect binding partners of C7, laminin-332 and integrin α6β4 were downregulated on protein level. Proteins that are involved in tissue repair such as fibronectin and tenascin C were upregulated, changes being indicative of increased TGF-β activity caused by disruption of integrin α6β4 signaling (27,28) and in line with increased *LTBP1* expression (Figure 2C).

Taken together, loss of C7 led to pronounced changes in the microenvironment of DEB keratinocytes. Especially, basement membrane components, direct and indirect binding partners of C7 were found to be downregulated while proteins that are involved in wound

12

healing were upregulated in DEB keratinocyte-derived ECM, largely consistent with transcriptome analyses.

Loss of C7 leads to an increase of inflammation markers

To distinguish transcriptional from translational or posttranslational regulation mechanisms, we directly analyzed the correlation between mRNA and protein abundance differences comparing DEB to control keratinocytes. The differences in gene expression and protein abundance of ECM proteins correlated only weakly (Figure 4A, r = 0.25, Pearson). Transcripts and proteins that were both downregulated in DEB keratinocytes display GO terms such as “extracellular region” and “cell adhesion” and are highlighted in yellow (Figure 4A). This group contains proteins associated with desmosomes like plakophilin 2 and integrin alpha-6, as well as protease inhibitors, i.e. cystatin A. Additional ECM proteins like laminin beta-1 and gamma-1 were identified as downregulated whereas respective mRNA levels did not correlate with the change in protein abundance, indicating perturbed posttranscriptional regulation mechanisms (Supplemental Figure S3). Downregulated transcripts of proteins that were upregulated in DEB are marked blue and are associated with GO terms “extracellular space”, “secreted” and “calcium ion binding”. Several annexins and S100 proteins, as well as calreticulin and cathepsin D belong to this group. Fibronectin was found to be upregulated on transcriptome and proteome level, similarly to corneodesmosin and filaggrin-2 (Figure 4A, marked red).

Interestingly, the proteins S100A8 and S100A9 displayed a marked increase in ECM of DEB keratinocytes compared to controls (log2 fold change >4) while showing only minimal regulation on mRNA level (Figure 4A-B, Welch's t-test, Permutation-based FDR 0.05). S100A8 and S100A9 often appear as calcium-binding heterodimer named calprotectin that has been used as biomarker for acute and chronic inflammation (29,30). Importantly, accumulation of S100A9 protein was also observed *in vivo* in the epidermis comparing immunofluorescence staining of DEB and control skin indicating that inflammation in DEB is promoted by keratinocytes (Figure 4C).

13

As transcriptome and ECM proteome analyses revealed complex and far reaching changes due to the loss of C7, we also analyzed the intracellular proteome of respective cells comparing DEB to control keratinocytes. Applying SILAC-based MS analysis 3,809 proteins were identified of which 2,054 could be quantified in all four samples (Supplemental Table S6, see Supplemental File S2 for annotated spectra of single peptide IDs). Also in this setting correlation of gene transcription and protein abundance was rather weak (Figure 4D; r = 0.19, Pearson), indicating that also in a disease model gene expression analyses cannot be employed to reliably infer protein abundances. Genes in each quadrant with a fold change >2 on protein and mRNA level were colored and selected enriched GO terms are shown. Again, loss of C7 had a dramatic influence on expression of genes involved in focal adhesion, hydroxylation and extracellular matrix. Intracellularly, S100A8 and S100A9 were less dysregulated, indicating that the extracellular abundance of both proteins may either be influenced through an increased translation coupled to an increased secretion, or a decreased extracellular degradation/increased stability in DEB (Figure 4B).

Keratins are the major intermediate filament proteins of epithelia and vital for mechanical stability (31). As we identified a significantly reduced expression of several keratin-encoding genes in DEB keratinocytes (Supplemental Figure S4), we analyzed keratin protein abundance in detail. Interestingly, only keratin 19 protein levels were significantly reduced in DEB cells (Supplemental Table S6). In contrast, intracellular proteins exhibiting known protein-protein interactions and being involved in regulation of apoptosis, ECM organization and collagen binding were significantly enriched in DEB cells indicating a perturbation on protein level of respective pathways (Supplemental Figure S5) (32,33).

Taken together, fold changes of mRNA and protein levels correlated weakly in primary human DEB and control keratinocytes, regardless if mRNA levels were compared to intracellular or extracellular protein abundances. Several proteins that are involved in inflammatory processes, such as S100A8 and S100A9 were only found to be upregulated on protein level indicating so far unknown, keratinocyte-intrinsic, posttranscriptional regulation mechanisms and characterizing keratinocytes as actively promoting inflammation in DEB.

14

Increased cathepsin B abundance and activity in C7 deficient DEB skin

To get a global impression of intracellular protein abundance differences induced by the loss of C7 we again performed a SOTA clustering and GO term enrichment analysis (Figure 5A, full list of GO terms in Supplemental Table S7). The GO terms “lysosome” and “endopeptidase activity” were found significantly enriched in a cluster containing highly abundant proteins in DEB cells. Indeed, several proteases were found to be significantly dysregulated in primary human DEB keratinocytes (Supplemental Table S8), the lysosomal proteases cathepsin Z and cathepsin B being significantly upregulated (Figure 5B-C, t-test, $p<0.05$). Higher abundance of the active forms of cathepsin B, the single-chain (SC) and heavy-chain enzyme (HC), in DEB keratinocytes was also shown by western blot analysis (Figure 5D). In conditioned DEB keratinocyte medium the proenzyme (PE) and the active single-chain enzyme were found enriched, suggesting a role of extracellular cathepsin B in ECM degradation (Figure 5E).

Higher protease abundance does not necessarily reflect higher protease activity, as this can be modulated by protease inhibitors (8). Interestingly the cathepsin B inhibitor cystatin A (CSTA) was found significantly depleted in DEB ECM, indicating an increased cathepsin B activity in DEB (Figure 3E). To directly measure the proteolytic activity of cathepsin B in cultured keratinocytes, cells were lysed and labelled with the substrate DCG-04, which targets active cysteine cathepsins (34). To distinguish cathepsin B from other active cysteine cathepsins the pan-cathepsin inhibitor E-64 and the cathepsin B-specific inhibitor Ca074 were used in control experiments prior to DCG-04 incubation to block the active center of proteases. Indeed, western blot analyses detecting protein-bound DCG-04 revealed significantly more active cathepsin B in DEB keratinocytes (Figure 5F-G). Orlowsi *et al.* conducted a similar cathepsin activity assays and characterized a western blot signal just above cathepsin B as cathepsin Z (35). Thus, also cathepsin Z appeared to be more active in DEB keratinocytes than in controls and might as well be involved in ECM degradation in DEB (Figure 5F).

Increased lysosomal protease abundance and activity might indicate a general increase in lysosomal protein degradation. Therefore, we assessed the activity of autophagy, an

15

intracellular degradation pathway targeting proteins and organelles for lysosomal degradation (36). By assaying accumulation of the lipidated autophagosomal marker protein MAP1LC3B (LC3-II) in the presence and absence of concanamycin A (ConA), an inhibitor of the lysosomal V-ATPase, we detected an increased autophagic capacity in DEB keratinocytes (Figure 5H-I), which is in line with increased cathepsin activity in DEB.

Finally, in agreement with the *in vitro* data, increased cathepsin B immunofluorescence staining was also observed in DEB skin compared to respective controls (Figure 5J). DEB skin revealed a particularly strong cathepsin B signal (green) in the blister roof and in the upper dermis. Taken together, an increase in cathepsin B abundance and activity as well as in autophagy was detected in DEB keratinocytes and skin, indicating a potential role of cathepsin B in DEB pathology as a mediator of both inflammation and activation of tissue-destabilizing proteolytic activities.

Increased cathepsin B levels depend on TGF-β-signaling and C7

TGF-β can induce *CTSB* expression *in vitro* in mouse cells (37) and was identified as increased in DEB skin and fibroblasts (8,9,11,38). To test if increased cathepsin B abundance in DEB keratinocytes also depends on TGF-β signaling, we analyzed *TGFB1* expression levels and activation of the TGF-β target proteins SMAD2/3. Indeed, *TGFB1* expression was significantly increased in DEB compared to control keratinocytes (Figure 6A) leading to increased SMAD2/3 phosphorylation (Figure 6B). Treatment of control keratinocytes with TGF-β led to a significant increase in cathepsin B levels (Figure 6C-D), and dual inhibition of TGF-β receptor type I/II with LY2109761 reduced cathepsin B levels in DEB keratinocytes (Figure 6E-F). Thus, increased TGF-β signaling contributes to increased cathepsin B levels and activity in DEB.

Finally, to test if increased cathepsin B abundance directly depends on the loss of C7, we made use of the fact that spontaneous restoration of *COL7A1* expression occurs in skin patches in a subset of DEB patients due to genetic reversion of the disease-causing mutation (so called revertant mosaicism (39)). In a biopsy specimen obtained from a reverted skin patch, C7 was present (Supplemental Figure S6). Critically, restoration of endogenous expression of

16

C7 led to a pronounced reduction in cathepsin B levels, indicating that C7 is sufficient to decrease cathepsin B levels (Figure 6G).

17

Discussion

Next to its important structural scaffold functions, the ECM is critical for cell homeostasis, proliferation and differentiation. Deficiency of the ECM protein C7 in DEB leads to substantial dermal changes: impaired skin regeneration and TGF-β-driven fibrosis that facilitates aggressive squamous cell carcinoma (SCC) (8-10,12,38,40). However, C7 is both a dermal and an epidermal product and so far the direct cellular changes that loss of C7 evokes in epidermal keratinocytes remained limitedly studied (7,38). A proteomic analysis of the skin of DEB mice suggested a cell-intrinsic injury-independent progression of fibrosis in DEB, the epidermis being a prime suspect for promoting this activity (11). In addition, dysfunctioning epithelia have emerged as instigators of fibrosis in other fibrotic diseases (13). The above led us to use DEB as a model to study the consequences of genetic loss of the structural protein C7 on epidermal cell homeostasis by comprehensive 'omics approaches'.

Intriguingly, the present study revealed dramatic changes in keratinocyte derived ECM as a consequence of loss of C7. Abundances of integrin α6β4, collagen XVII and laminin-332, indirect and direct ligands of C7, were reduced (Figure 7). Integrin α6β4 and collagen XVII are transmembrane proteins that bind laminin-332 in the basement membrane (BM). Laminin-332 and collagen XVII form anchoring filaments that are attached to C7-containing anchoring fibrils (41,42), which provide functional integrity of the dermal-epidermal junction zone (DEJZ) by connecting the collagen IV network of the BM to dermal collagen fibrils (Figure 7) (43-45). Our findings suggest that loss of epidermal C7 leads to a global modification and destabilization of the DEJZ (46). Fibronectin was found to be strongly increased in ECM of DEB keratinocytes indicating a wound-like phenotype, at least *in vitro* (38,47). Importantly, the integrin $\alpha 6\beta 4$ receptor was shown to be a negative regulator of TGF-β expression and inversely increased TGF-β activity in keratinocytes may cause reduction of laminin-332 and integrin $\alpha 6\beta 4$ and upregulation of proteins associated with tissue damage (27,28). Thus, increased TGF-β signaling due to the loss of repression may lead to many of the changes observed in our global analysis.

18

To identify potential transcriptional or posttranscriptional regulation of protein abundances, we compared fold changes of mRNA to fold changes of protein abundance in DEB and control keratinocytes. Protein and mRNA abundances correlated rather weakly, corroborating the finding that under steady-state conditions protein abundances are mainly controlled by posttranscriptional mechanisms such as rate of protein translation and protein degradation (48,49). Surprisingly intra- and extracellular protein levels correlated similarly with respective mRNA levels indicating that in keratinocytes – once an extracellular protein is synthesized – protein secretion follows swiftly and is regulated on a global level for the majority of proteins. Underlying molecular mechanisms will have to be addressed in detail in future studies.

The above analyses identified hitherto unknown dysregulated pathways in DEB keratinocytes. Several proteins were found to be regulated in the cellular microenvironment without showing significant changes of respective mRNA levels (Figure 7). For example, S100A8 and S100A9, forming the calcium-binding heterodimer calprotectin, were identified as upregulated keratinocyte-products in DEB. Both proteins have been previously found upregulated in non-healing human skin wounds (50), and in acute mouse and human wounds, keratinocytes being the expressing cell type (51). Also, in inflammatory conditions, such as rheumatoid arthritis and abscesses, both marker proteins were identified as increased (52). The strongly upregulated keratinocyte-derived S100A8 and S100A9 might be interesting druggable targets to interfere with the persisting inflammation of DEB skin. Synthetic inhibitors called peptibodies (peptide–Fc fusion proteins) directed against S100A8 and S100A9 have been shown to interfere with their activity in mice (53).

Intracellular proteome changes due to the loss of C7 were extensive. Proteins carrying the GO-terms vesicle-mediated transport, lysosome and endopeptidase activity were significantly enriched in DEB keratinocytes indicating a dysregulation of proteolytic processes. In line, autophagy was identified as significantly upregulated in DEB keratinocytes, which is in stark contrast to DEB fibroblasts (10). Of the significantly enriched proteases, cathepsins B and Z are of high interest as they can cleave ECM proteins, interfere with cell-matrix contacts and activate TGF-β signaling (54-57). Thus, they may play a role in the detachment of epidermis

19

and dermis, and contribute to fibrosis in DEB. Importantly, spontaneously gene-corrected mosaic keratinocytes from a DEB patient demonstrated that cathepsin B levels correlated inversely with C7 levels. The fact that cathepsin B levels were regulated by TGF-β suggests a detrimental positive feedback loop: loss of C7 leads to increased TGF-β signaling, increasing cathepsin B levels, which in turn may potentiate TGF-β signals (Figure 7). The causality, kinetic regulation of events, as well as the regulation in human skin *in vivo* will have to be addressed in future studies.

In situ validation revealed a clear increase of cathepsin B in DEB skin, supporting an *in vivo* role of cathepsin B in the blister phenotype in DEB. Active cathepsin B might also contribute to posttranscriptional regulation of ECM proteins in DEB, such as the decrease of laminins beta-1 and gamma-1 (Figure 7). Increased activity of matrix metalloprotease 1 (MMP1), produced by skin fibroblasts, has been suggested to play a role in the blister phenotype of DEB (58). Here we show that also keratinocytes may contribute to excessive ECM degradation via an increased cathepsin abundance and activity.

Secreted cathepsins have been implicated in keratinocyte migration (59) and wound healing (60). In line with this, cathepsins B and Z have also been shown to promote tumor progression in various mouse models of human cancers (61). Consequently, various approaches for cathepsin inhibition in cancers are currently investigated, as “stand alone” or part of combinatory therapy approaches (for review: (62)). As DEB patients often develop aggressive SCC, cathepsins B and Z might also be promising druggable targets in DEB.

Taken together, by applying a comprehensive approach combining SILAC-based quantitative MS with next generation RNA sequencing followed by bioinformatics analyses we generated a global, yet detailed picture of dysregulated molecular consequences of C7-deficiency. Our study revealed that loss of C7 from epidermal keratinocytes evokes cell-intrinsic wound healing-like responses. These epidermal activities establish a TGF-β-driven, pro-inflammatory and tissue destabilizing micromilieu enabling development of keratinocyte-promoted fibrosis in the dermis. Thus, by uncovering epidermal dysregulation as a catalyst of dermal fibrosis our study identifies potential new drug targets for design of new treatment strategies for DEB.

20

Importantly, it may also provide insights into the pathogenesis of other conditions dependent on chronic, uninhibited TGF-β signaling, associated with scarring and fibrosis.

21

Supplemental Information

Supplemental Information can be found with this article online.

Author Contributions

Conceptualization, KT, AN, TR, LBT, and JD; Methodology, KT, BAG, OB, AE, JL, IA, EW, DK, AN, TR, RB, CH, LBT, and JD; Investigation, KT, BAG, OB, AE, JL, IA; Writing – Original draft, KT, TR, CH, LBT and JD; Writing – Review & Editing, KT, TR, AN, CH, LBT and JD; Funding Acquisition, Resources, & Supervision, AN, DK, TR, RB, CH, LBT and JD.

Acknowledgments

We thank the Freiburg Galaxy Platform for bioinformatics support (https://galaxy.uni-freiburg.de/). This work was supported by the German Research Foundation (DFG) through the CRC 992 (RB), CRC 850 (LBT, TR, JD), DE 1757/3-2 (JD), NY90/2-1, NY90/3-2 (AN), KI1795/1-1 (DK), by the German Federal Ministry of Education and Research (BMBF) grant 031A538A (RB), under the frame of Erare-4, by the ERA-Net for Research on Rare Diseases (EBThera; LBT), by the Excellence Initiative of the German Federal and State Governments through EXC 294 BIOSS (TR, RB, LBT, JD), and by the Swiss National Science Foundation, grant 31003A-166482/1 (JD).

References

1. Hynes, R. O. (2009) The extracellular matrix: not just pretty fibrils. *Science* **326**, 1216-1219
2. Pozzi, A., Yurchenco, P. D., and Iozzo, R. V. (2016) The nature and biology of basement membranes. *Matrix Biol*
3. Bonnans, C., Chou, J., and Werb, Z. (2014) Remodelling the extracellular matrix in development and disease. *Nat Rev Mol Cell Biol* **15**, 786-801
4. Has, C., and Nystrom, A. (2015) Epidermal Basement Membrane in Health and Disease. *Curr Top Membr* **76**, 117-170
5. Fine, J. D., Eady, R. A., Bauer, E. A., Bauer, J. W., Bruckner-Tuderman, L., Heagerty, A., Hintner, H., Hovnanian, A., Jonkman, M. F., Leigh, I., et al. (2008) The classification of inherited epidermolysis bullosa (EB): Report of the Third International Consensus Meeting on Diagnosis and Classification of EB. *J Am Acad Dermatol* **58**, 931-950
6. Dayal, J. H., Cole, C. L., Pourreyron, C., Watt, S. A., Lim, Y. Z., Salas-Alanis, J. C., Murrell, D. F., McGrath, J. A., Stieger, B., Jahoda, C., et al. (2014) Type VII collagen regulates expression of OATP1B3, promotes front-to-rear polarity and increases

22

structural organisation in 3D spheroid cultures of RDEB tumour keratinocytes. *J Cell Sci* **127**, 740-751
7. Watt, S. A., Pourreyron, C., Purdie, K., Hogan, C., Cole, C. L., Foster, N., Pratt, N., Bourdon, J. C., Appleyard, V., Murray, K., et al. (2011) Integrative mRNA profiling comparing cultured primary cells with clinical samples reveals PLK1 and C20orf20 as therapeutic targets in cutaneous squamous cell carcinoma. *Oncogene* **30**, 4666-4677
8. Kuttner, V., Mack, C., Rigbolt, K. T., Kern, J. S., Schilling, O., Busch, H., Bruckner-Tuderman, L., and Dengjel, J. (2013) Global remodelling of cellular microenvironment due to loss of collagen VII. *Mol Syst Biol* **9**, 657
9. Ng, Y. Z., Pourreyron, C., Salas-Alanis, J. C., Dayal, J. H., Cepeda-Valdes, R., Yan, W., Wright, S., Chen, M., Fine, J. D., Hogg, F. J., et al. (2012) Fibroblast-derived dermal matrix drives development of aggressive cutaneous squamous cell carcinoma in patients with recessive dystrophic epidermolysis bullosa. *Cancer Res* **72**, 3522-3534
10. Kuttner, V., Mack, C., Gretzmeier, C., Bruckner-Tuderman, L., and Dengjel, J. (2014) Loss of collagen VII is associated with reduced transglutaminase 2 abundance and activity. *J Invest Dermatol* **134**, 2381-2389
11. Nystrom, A., Thriene, K., Mittapalli, V., Kern, J. S., Kiritsi, D., Dengjel, J., and Bruckner-Tuderman, L. (2015) Losartan ameliorates dystrophic epidermolysis bullosa and uncovers new disease mechanisms. *EMBO Mol Med* **7**, 1211-1228
12. Odorisio, T., Di Salvio, M., Orecchia, A., Di Zenzo, G., Piccinni, E., Cianfarani, F., Travaglione, A., Uva, P., Bellei, B., Conti, A., et al. (2014) Monozygotic twins discordant for recessive dystrophic epidermolysis bullosa phenotype highlight the role of TGF-beta signalling in modifying disease severity. *Hum Mol Genet* **23**, 3907-3922
13. Sakai, N., and Tager, A. M. (2013) Fibrosis of two: Epithelial cell-fibroblast interactions in pulmonary fibrosis. *Biochim Biophys Acta* **1832**, 911-921
14. Kern, J. S., Gruninger, G., Imsak, R., Muller, M. L., Schumann, H., Kiritsi, D., Emmert, S., Borozdin, W., Kohlhase, J., Bruckner-Tuderman, L., et al. (2009) Forty-two novel COL7A1 mutations and the role of a frequent single nucleotide polymorphism in the MMP1 promoter in modulation of disease severity in a large European dystrophic epidermolysis bullosa cohort. *Br J Dermatol* **161**, 1089-1097
15. Kern, J. S., Kohlhase, J., Bruckner-Tuderman, L., and Has, C. (2006) Expanding the COL7A1 mutation database: novel and recurrent mutations and unusual genotype-phenotype constellations in 41 patients with dystrophic epidermolysis bullosa. *J Invest Dermatol* **126**, 1006-1012
16. Myllyharju, J., and Kivirikko, K. I. (2004) Collagens, modifying enzymes and their mutations in humans, flies and worms. *Trends Genet* **20**, 33-43
17. Vlodavsky, I. (2001) Preparation of extracellular matrices produced by cultured corneal endothelial and PF-HR9 endodermal cells. *Curr Protoc Cell Biol* **Chapter 10**, Unit 10 14
18. Wisniewski, J. R., Zougman, A., Nagaraj, N., and Mann, M. (2009) Universal sample preparation method for proteome analysis. *Nat Methods* **6**, 359-362
19. Shevchenko, A., Tomas, H., Havlis, J., Olsen, J. V., and Mann, M. (2006) In-gel digestion for mass spectrometric characterization of proteins and proteomes. *Nat Protoc* **1**, 2856-2860
20. Rappsilber, J., Mann, M., and Ishihama, Y. (2007) Protocol for micro-purification, enrichment, pre-fractionation and storage of peptides for proteomics using StageTips. *Nat Protoc* **2**, 1896-1906
21. Cox, J., and Mann, M. (2008) MaxQuant enables high peptide identification rates, individualized p.p.b.-range mass accuracies and proteome-wide protein quantification. *Nat Biotechnol* **26**, 1367-1372
22. Vizcaino, J. A., Csordas, A., del-Toro, N., Dianes, J. A., Griss, J., Lavidas, I., Mayer, G., Perez-Riverol, Y., Reisinger, F., Ternent, T., et al. (2016) 2016 update of the PRIDE database and its related tools. *Nucleic Acids Res* **44**, D447-456
23. Saharinen, J., and Keski-Oja, J. (2000) Specific sequence motif of 8-Cys repeats of TGF-beta binding proteins, LTBPs, creates a hydrophobic interaction surface for binding of small latent TGF-beta. *Mol Biol Cell* **11**, 2691-2704

23

24. Geiger, T., Cox, J., Ostasiewicz, P., Wisniewski, J. R., and Mann, M. (2010) Super-SILAC mix for quantitative proteomics of human tumor tissue. *Nat Methods* **7**, 383-385
25. Naba, A., Clauser, K. R., Hoersch, S., Liu, H., Carr, S. A., and Hynes, R. O. (2012) The matrisome: in silico definition and in vivo characterization by proteomics of normal and tumor extracellular matrices. *Mol Cell Proteomics* **11**, M111 014647
26. Huang da, W., Sherman, B. T., and Lempicki, R. A. (2009) Systematic and integrative analysis of large gene lists using DAVID bioinformatics resources. *Nat Protoc* **4**, 44-57
27. Rodius, S., Indra, G., Thibault, C., Pfister, V., and Georges-Labouesse, E. (2007) Loss of alpha6 integrins in keratinocytes leads to an increase in TGFbeta and AP1 signaling and in expression of differentiation genes. *J Cell Physiol* **212**, 439-449
28. Tsuruta, D., Kobayashi, H., Imanishi, H., Sugawara, K., Ishii, M., and Jones, J. C. (2008) Laminin-332-integrin interaction: a target for cancer therapy? *Curr Med Chem* **15**, 1968-1975
29. Herrera, O. R., Christensen, M. L., and Helms, R. A. (2016) Calprotectin: Clinical Applications in Pediatrics. *J Pediatr Pharmacol Ther* **21**, 308-321
30. Burri, E., and Beglinger, C. (2012) Faecal calprotectin -- a useful tool in the management of inflammatory bowel disease. *Swiss Med Wkly* **142**, w13557
31. Moll, R., Divo, M., and Langbein, L. (2008) The human keratins: biology and pathology. *Histochem Cell Biol* **129**, 705-733
32. Knaup, J., Verwanger, T., Gruber, C., Ziegler, V., Bauer, J. W., and Krammer, B. (2012) Epidermolysis bullosa - a group of skin diseases with different causes but commonalities in gene expression. *Exp Dermatol* **21**, 526-530
33. Maier, K., He, Y., Wolfle, U., Esser, P. R., Brummer, T., Schempp, C., Bruckner-Tuderman, L., and Has, C. (2016) UV-B-induced cutaneous inflammation and prospects for antioxidant treatment in Kindler syndrome. *Hum Mol Genet* **25**, 5339-5352
34. Greenbaum, D., Medzihradszky, K. F., Burlingame, A., and Bogyo, M. (2000) Epoxide electrophiles as activity-dependent cysteine protease profiling and discovery tools. *Chem Biol* **7**, 569-581
35. Orlowski, G. M., Colbert, J. D., Sharma, S., Bogyo, M., Robertson, S. A., and Rock, K. L. (2015) Multiple Cathepsins Promote Pro-IL-1beta Synthesis and NLRP3-Mediated IL-1beta Activation. *J Immunol* **195**, 1685-1697
36. Gretzmeier, C., Eiselein, S., Johnson, G. R., Engelke, R., Nowag, H., Zarei, M., Kuttner, V., Becker, A. C., Rigbolt, K. T. G., Hoyer-Hansen, M., et al. (2017) Degradation of protein translation machinery by amino acid starvation-induced macroautophagy. *Autophagy*, 1064-1075
37. Jiang, Y., Woosley, A. N., Sivalingam, N., Natarajan, S., and Howe, P. H. (2016) Cathepsin-B-mediated cleavage of Disabled-2 regulates TGF-beta-induced autophagy. *Nat Cell Biol* **18**, 851-863
38. Nystrom, A., Velati, D., Mittapalli, V. R., Fritsch, A., Kern, J. S., and Bruckner-Tuderman, L. (2013) Collagen VII plays a dual role in wound healing. *J Clin Invest* **123**, 3498-3509
39. Kiritsi, D., Valari, M., Michos, A., Karakosta, V., and Has, C. (2016) The mysteries of mosaicism: phenotypic variability in a family with incontinentia pigmenti. *Eur J Dermatol* **26**, 504-506
40. Watt, S. A., Dayal, J. H., Wright, S., Riddle, M., Pourreyron, C., McMillan, J. R., Kimble, R. M., Prisco, M., Gartner, U., Warbrick, E., et al. (2015) Lysyl Hydroxylase 3 Localizes to Epidermal Basement Membrane and Is Reduced in Patients with Recessive Dystrophic Epidermolysis Bullosa. *PLoS One* **10**, e0137639
41. de Pereda, J. M., Ortega, E., Alonso-Garcia, N., Gomez-Hernandez, M., and Sonnenberg, A. (2009) Advances and perspectives of the architecture of hemidesmosomes: lessons from structural biology. *Cell Adh Migr* **3**, 361-364
42. Walko, G., Castanon, M. J., and Wiche, G. (2015) Molecular architecture and function of the hemidesmosome. *Cell Tissue Res* **360**, 529-544

24

43. Villone, D., Fritsch, A., Koch, M., Bruckner-Tuderman, L., Hansen, U., and Bruckner, P. (2008) Supramolecular interactions in the dermo-epidermal junction zone: anchoring fibril-collagen VII tightly binds to banded collagen fibrils. *J Biol Chem* **283**, 24506-24513
44. Chung, H. J., and Uitto, J. (2010) Type VII collagen: the anchoring fibril protein at fault in dystrophic epidermolysis bullosa. *Dermatol Clin* **28**, 93-105
45. Nystrom, A., Bornert, O., and Kuhl, T. (2016) Cell therapy for basement membrane-linked diseases. *Matrix Biol*
46. Bremer, J., Bornert, O., Nystrom, A., Gostynski, A., Jonkman, M. F., Aartsma-Rus, A., van den Akker, P. C., and Pasmooij, A. M. (2016) Antisense Oligonucleotide-mediated Exon Skipping as a Systemic Therapeutic Approach for Recessive Dystrophic Epidermolysis Bullosa. *Mol Ther Nucleic Acids* **5**, e379
47. Fritsch, A., Loeckermann, S., Kern, J. S., Braun, A., Bosl, M. R., Bley, T. A., Schumann, H., von Elverfeldt, D., Paul, D., Erlacher, M., et al. (2008) A hypomorphic mouse model of dystrophic epidermolysis bullosa reveals mechanisms of disease and response to fibroblast therapy. *J Clin Invest* **118**, 1669-1679
48. Vogel, C., and Marcotte, E. M. (2012) Insights into the regulation of protein abundance from proteomic and transcriptomic analyses. *Nat Rev Genet* **13**, 227-232
49. Schwanhausser, B., Busse, D., Li, N., Dittmar, G., Schuchhardt, J., Wolf, J., Chen, W., and Selbach, M. (2011) Global quantification of mammalian gene expression control. *Nature* **473**, 337-342
50. Eming, S. A., Koch, M., Krieger, A., Brachvogel, B., Kreft, S., Bruckner-Tuderman, L., Krieg, T., Shannon, J. D., and Fox, J. W. (2010) Differential proteomic analysis distinguishes tissue repair biomarker signatures in wound exudates obtained from normal healing and chronic wounds. *J Proteome Res* **9**, 4758-4766
51. Thorey, I. S., Roth, J., Regenbogen, J., Halle, J. P., Bittner, M., Vogl, T., Kaesler, S., Bugnon, P., Reitmaier, B., Durka, S., et al. (2001) The Ca2+-binding proteins S100A8 and S100A9 are encoded by novel injury-regulated genes. *J Biol Chem* **276**, 35818-35825
52. Yui, S., Nakatani, Y., and Mikami, M. (2003) Calprotectin (S100A8/S100A9), an inflammatory protein complex from neutrophils with a broad apoptosis-inducing activity. *Biol Pharm Bull* **26**, 753-760
53. Qin, H., Lerman, B., Sakamaki, I., Wei, G., Cha, S. C., Rao, S. S., Qian, J., Hailemichael, Y., Nurieva, R., Dwyer, K. C., et al. (2014) Generation of a new therapeutic peptide that depletes myeloid-derived suppressor cells in tumor-bearing mice. *Nat Med* **20**, 676-681
54. Akkari, L., Gocheva, V., Kester, J. C., Hunter, K. E., Quick, M. L., Sevenich, L., Wang, H. W., Peters, C., Tang, L. H., Klimstra, D. S., et al. (2014) Distinct functions of macrophage-derived and cancer cell-derived cathepsin Z combine to promote tumor malignancy via interactions with the extracellular matrix. *Genes Dev* **28**, 2134-2150
55. Bengsch, F., Buck, A., Gunther, S. C., Seiz, J. R., Tacke, M., Pfeifer, D., von Elverfeldt, D., Sevenich, L., Hillebrand, L. E., Kern, U., et al. (2014) Cell type-dependent pathogenic functions of overexpressed human cathepsin B in murine breast cancer progression. *Oncogene* **33**, 4474-4484
56. Gogineni, V. R., Gupta, R., Nalla, A. K., Velpula, K. K., and Rao, J. S. (2012) uPAR and cathepsin B shRNA impedes TGF-beta1-driven proliferation and invasion of meningioma cells in a XIAP-dependent pathway. *Cell Death Dis* **3**, e439
57. Moles, A., Tarrats, N., Fernandez-Checa, J. C., and Mari, M. (2012) Cathepsin B overexpression due to acid sphingomyelinase ablation promotes liver fibrosis in Niemann-Pick disease. *J Biol Chem* **287**, 1178-1188
58. Colombi, M., Gardella, R., Zoppi, N., Moro, L., Marini, D., Spurr, N. K., and Barlati, S. (1992) Exclusion of stromelysin-1, stromelysin-2, interstitial collagenase and fibronectin genes as the mutant loci in a family with recessive epidermolysis bullosa dystrophica and a form of cerebellar ataxia. *Hum Genet* **89**, 503-507
59. Buth, H., Wolters, B., Hartwig, B., Meier-Bornheim, R., Veith, H., Hansen, M., Sommerhoff, C. P., Schaschke, N., Machleidt, W., Fusenig, N. E., et al. (2004) HaCaT

25

keratinocytes secrete lysosomal cysteine proteinases during migration. *Eur J Cell Biol* **83**, 781-795
60. Buth, H., Luigi Buttigieg, P., Ostafe, R., Rehders, M., Dannenmann, S. R., Schaschke, N., Stark, H. J., Boukamp, P., and Brix, K. (2007) Cathepsin B is essential for regeneration of scratch-wounded normal human epidermal keratinocytes. *Eur J Cell Biol* **86**, 747-761
61. Reinheckel, T., Peters, C., Kruger, A., Turk, B., and Vasiljeva, O. (2012) Differential Impact of Cysteine Cathepsins on Genetic Mouse Models of De novo Carcinogenesis: Cathepsin B as Emerging Therapeutic Target. *Front Pharmacol* **3**, 133
62. Olson, O. C., and Joyce, J. A. (2015) Cysteine cathepsin proteases: regulators of cancer progression and therapeutic response. *Nat Rev Cancer* **15**, 712-729

26

Figure Legends:

Figure 1: Loss of C7 in DEB is associated with skin fragility, inflammation and scarring. (A) Anti-C7 western blot. C7 is deficient in the ECM isolated from cultured primary DEB keratinocytes derived from depicted patients. **(B) Clinical phenotypes of DEB.** Loss of C7 is associated with skin fragility, inflammation and scarring. The age of patient is indicated.

Figure 2: Gene expression changes in primary DEB keratinocytes. (A) Altered gene expression in DEB keratinocytes. Cluster analysis of 300 differentially regulated genes in DEB keratinocytes (BH corrected q-value 0.1) as determined by next generation sequencing. TPM values were log2-transformed and z-score normalized. Columns containing data from the different samples were hierarchically clustered and rows containing gene entries were clustered by k-means. Data separated into 5 clusters showing clear differences between DEB and control cells (Ctrl). **(B) Functional annotation of significantly regulated genes in DEB cells.** Differentially expressed genes in DEB are significantly enriched in the shown processes (BH corrected q-value 0.05). Loss of C7 affects transcription of genes involved in cell migration and ECM organization. **(C) Examples of dysregulated gene expression in DEB.** Bar graphs show transcript abundances (TPM values) of differentially expressed genes. Expression of genes encoding direct and indirect binding partners of C7 (*LAMA3/LAMB3/LAMC2, ITGA6/ITGB4*) were found to be downregulated in DEB keratinocytes while the transcript encoding LTBP1 was more abundant in DEB keratinocytes.

Figure 3: Analysis of the extracellular proteome of DEB keratinocytes. (A) Cell culture scheme. Keratinocytes were kept in culture for six days. Fresh culture medium containing ascorbate was added daily. The ECM was harvested at day 6 using 4% SDS. **(B) Analysis of ECM isolation procedure.** Western blot analyses were performed to address the quality of ECM isolation. Intracellular proteins representing the cell compartments nucleus (TBP), Golgi apparatus (GOLGA1), endoplasmic reticulum (HSPA5) and cytosol (GAPDH) were only

27

detected in whole cell lysate (WCL). ECM proteins such as collagen XVII (COL17A1), C7 as well as fibronectin (FN1) and tenascin C (TNC) were found in both, WCL and ECM. **(C) SILAC-based quantitative MS workflow.** Medium and heavy SILAC-labeled cells were mixed with a light-labeled standard 1:1:1 and samples were processed as outlined. The resulting peptide mixtures were analyzed by LC-MS/MS. In total 2 biological replicates of 2 DEB and control cells, each, were analyzed. **(D) SOTA clustering of proteins quantified in ECM of DEB and control cells.** ECM proteins were filtered bioinformatically and respective protein ratios were log2-transformed and z-score normalized. Proteins in each cluster were tested by DAVID for enriched GO terms (biological process (BP), cellular compartment (CC)). Selected terms are shown (full list in Supplemental Table S5). **(E) Network analysis of significantly regulated proteins**. STRING DB was used to identify protein-protein interactions of significantly regulated proteins (confidence score 0.4). Known C7 binding partners, such as integrin α6β4 and laminin-332 were significantly downregulated in ECM isolated from DEB keratinocytes, whereas proteins involved in fibrosis and inflammation were significantly upregulated (Welch's t-test, Permutation-based FDR 0.05). The figure was produced using Servier Medical Art.

Figure 4: Gene expression and protein abundance correlate only weakly in primary keratinocytes. (A) Correlation of gene transcription and ECM protein abundance. Gene expression and protein abundance only correlate weakly (r = 0.25). Genes showing a twofold change on RNA and protein level were highlighted and tested by DAVID for GO enrichment. Selected terms are shown. S100A8 and A9 were significantly regulated on protein level but not on mRNA level. **(B) Relative mRNA and protein abundances of S100A8 and S100A9.** Relative values compared to the respective control 1 (Ctrl 1) are shown. Protein levels were significantly higher (Welch's t-test, Permutation-based FDR 0.05) in ECM isolated of DEB cells compared to controls, while mRNA levels did not change significantly. **(C) *In vivo* accumulation of S100A9.** Immunofluorescence staining of DEB skin reveals a strong increase of S100A9 in the epidermis (green signal). Blue = DAPI staining. **(D) Correlation of gene transcription and intracellular protein abundance.** Gene expression and protein

28

abundance correlated weakly (r=0.19). Genes in each quadrant with a fold change > 2 on mRNA and protein level were colored and tested by DAVID for GO enrichment (biological process (BP), cellular compartment (CC), molecular function (MF) and SP_PIR_KEYWORDS (KW)). Selected terms are shown.

Figure 5: Increased cathepsin B abundance and activity in DEB keratinocytes. (A) Cluster analysis of intracellular protein abundances. SOTA clustering of intracellular proteins that were quantified in DEB keratinocytes compared to controls. Protein ratios were log2-transformed and z-score normalized. Proteins in each cluster were tested by DAVID for enriched GO terms (biological process (BP), cellular compartment (CC) and molecular function (MF). Selected terms are shown (full list in Supplemental Table S7). **(B-C) Protein abundance measurements.** Protein abundances of cathepsin B (B) and cathepsin Z (C) were significantly higher in DEB compared to control keratinocytes as determined by SILAC-based, quantitative MS (t-test, two-tailed, two-sample equal variance, $p<0.05$). a and b: biological replicates of indicated primary cells analyzed by swapped SILAC labels. **(D-E) Western blot analysis revealed higher amounts of cathepsin B in DEB keratinocytes.** Higher abundance of the cathepsin B single-chain enzyme (SC) and the heavy chain of the two-chain enzyme (HC) were detected in DEB whole cell lysates of independent biological replicates by western blot (D). In conditioned keratinocyte medium increased amounts of proenzyme (PE) and active cathepsin B (HC form) were detected under DEB conditions (E). **(F) Cathepsin B activity assays revealed more active cathepsin B in DEB keratinocytes.** Bands corresponding to active cathepsins B and Z are highlighted by arrows and triangles, respectively. Biotin-DCG-04 was detected using fluorescently labeled streptavidin. DCG-04: substrate of cysteine cathepsins, E-64: cysteine protease inhibitor, Ca074: cathepsin B inhibitor, 95°C (neg. control): samples were denaturated prior DCG-04 incubation in order to reveal unspecific binding. **(G) Quantification of activity blots**. Four independently performed activity assays as shown in (F) were quantified by imageJ revealing significantly more active cathepsin B in DEB keratinocytes (t-test, two-tailed, two-sample equal variance: $p<0.001$). ACTB values (AU) were

29

used for normalization. **(H-I) Increased autophagic flux in DEB keratinocytes.** Regulation of lipidated MAP1LC3B (LC3-II), an autophagosomal marker protein, was analyzed in control and DEB keratinocytes plus/minus concanamycin A (ConA), an inhibitor of the lysosomal V-ATPase, by western blot (H). Quantification of ConA treated samples compared to untreated samples revealed an increased autophagic flux in DEB keratinocytes (*: $p<0.05$, T test, n=3). **(J) Increased cathepsin B levels in DEB skin.** Immunofluorescence staining of DEB skin revealed a strongly increased cathepsin B signal (green) at the blister roof and in the upper dermis. In healthy control skin cathepsin B occured mainly at the dermal-epidermal junction and the upper dermis, showing a weaker signal. Blue = DAPI staining.

Figure 6: TGF-β-dependent increase of cathepsin B levels. (A) Increased expression of *TGFB1* in primary DEB keratinocytes. qPCRs testing *TGFB1* expression levels were performed on mRNA isolated from primary DEB and Ctrl keratinocytes (n=9). Expression levels were normalized to GAPDH expression. **: $P<0.01$, T-Test. **(B) Increased activity of TGF-β1 in primary DEB keratinocytes.** TGF-β1-responsive phosphorylation events of SMAD2/3 were analyzed by phosphosite-specific antibodies (SMAD2 phospho-Ser465/467; SMAD3 phospho-Ser423/425). Actin (ACTB) was used as loading control. **(C-D) TGF-β treatment led to increased cathepsin B levels.** Control keratinocytes (immortalized using the HPV E6/E7 genes) were incubated with 10 ng/mL TGF-β1 for 48 h and cathepsin B levels were assessed by western blot (C). TGF-β1 treatment led to a significant increase in cathepsin B levels (D) (paired T-test, $p<0.05$; n = 4). Beta tubulin (TUBB) was used as loading control and increased SMAD2/3 phosphorylation as positive control for increased TGF-β1 stimulation. **(E-F) TGF-β inhibition led to decreased cathepsin B levels in DEB cells.** DEB keratinocytes (immortalized using the HPV E6/E7 genes) were incubated with 4.4 μg/mL LY2109761 for 48 h and cathepsin B levels were assessed by western blot (E). Inhibition of TGF-β receptor type I/II led to a significant decrease in cathepsin B levels (F) (paired T-test, $p<0.05$; n = 4). Beta tubulin was used as loading control and decreased SMAD2/3 phosphorylation as positive

30

control for inhibition of TGF-β signaling. **(G) C7 leads to decreased cathepsin B levels.** Conditioned medium (CM) and cell lysates of primary reverted DEB cells showing a natural expression of C7 were analyzed by western blot on cathepsin B level. TUBB served as loading control for cell lysates. SC: Cathepsin B single-chain enzyme; HC: heavy chain of the two-chain enzyme; PE: proenzyme (PE).

Figure 7: Model of perturbed protein homeostasis in DEB. In normal skin, C7 is present and active in the extracellular environment. It may also be sensed intracellularly. In DEB skin**,** the lack of extracellular C7 leads to the loss of direct and indirect extracellular binding partners, like laminin-332 and integrin α6β4, contributing to increased TGF-β signaling by a loss of repression. Increased TGF-β leads to increased abundance and secretion of cathepsin B, which in turn may further release extracellular TGF-β in a positive feedback mechanism. Increased cathepsin B levels also depend on the presence of C7 by a so far unknown mechanism. In parallel, the levels of inflammatory proteins, like S100A8 and S100A9, are increased. Extracellular cathepsin B may further contribute to DEB pathology by degrading the ECM at the dermal-epidermal junction, e.g. laminin beta-1 and gamma-1 present in laminin 311 and laminin 511, and collagen IV (8), weakening the basement membrane.

31

Tables

Table 1: Characteristics of primary DEB cells used in this study. n.d.: not detected.

ID	Age at biopsy / gender	*COL7A1* mutation	C7 levels (IF analysis)	References (report of patients)
DEB 1	8 years/m	c.1934delC c.1934delC	n.d.	(15)
DEB 2	1 month/f	c.425A>G c.682+1G>A	n.d.	(15)
DEB 3	1 month/m	c.425A>G c.5261dupC	n.d.	(14)
DEB 4	6 years/f	c.425A>G c.682+1G>A	n.d.	Patient not reported before
DEB 5	1 month/f	c.4119+1G>C c.8523_8536del	n.d.	Patient not reported before
DEB 6	3 years/f	c.682+1G>A c.5261dupC	n.d.	Patient not reported before
DEB 7	1 month/f	c.425A>G c.425A>G	n.d.	(15)
DEB 8	30 years/m	c.426+1G>A c.1474del11	n.d.	(15)
DEB 9	53 years/m	c.425A>G c.425A>G	n.d.	Patient not reported before
DEB 10	47 years/m	c.425A>G c.425A>G	n.d.	Patient not reported before

32

Table 2: Characteristics of primary control cells used in this study.

ID	Age at biopsy/ gender
Ctrl 1	2 years/m
Ctrl 2	4 years/m
Ctrl 3	3 years/m
Ctrl 4	20 years/f
Ctrl 5	13 years/f
Ctrl 6	1 year/m
Ctrl 7	38 years/f
Ctrl 8	4 years/m
Ctrl 9	6 years/m
Ctrl 10	34 years/f
Ctrl 11	13 years/f
Ctrl 12	1 years/m

33

Figure 1

34

Figure 2

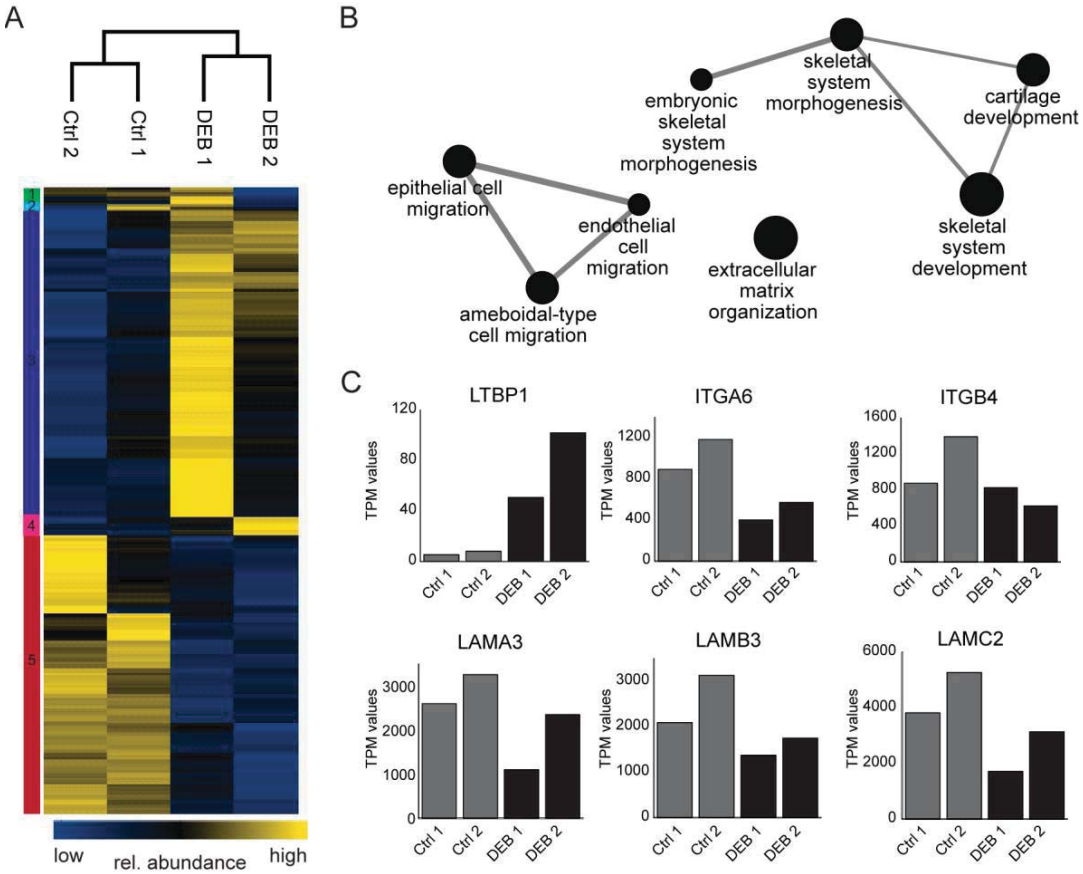

35

Figure 3

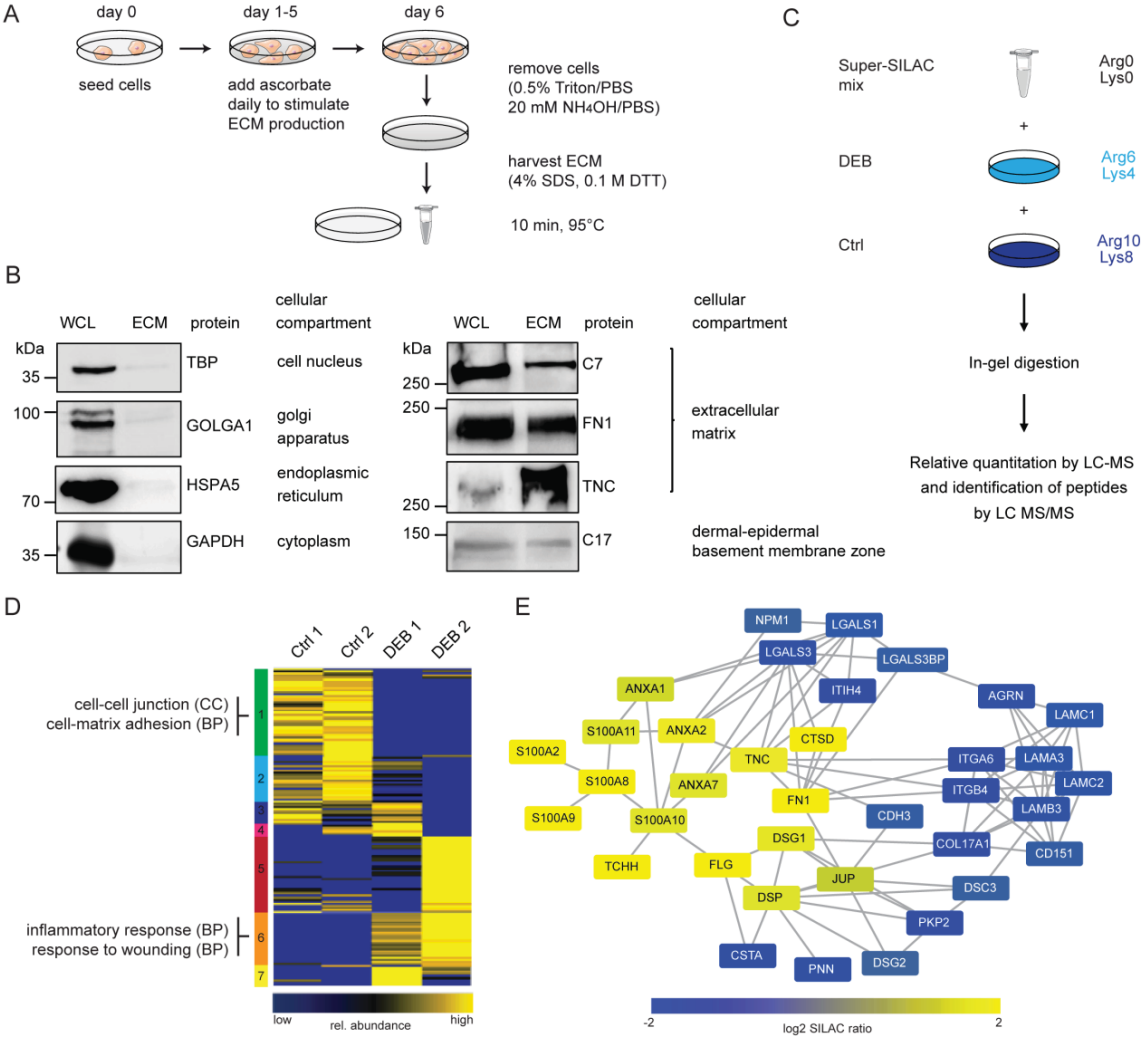

36

Figure 4

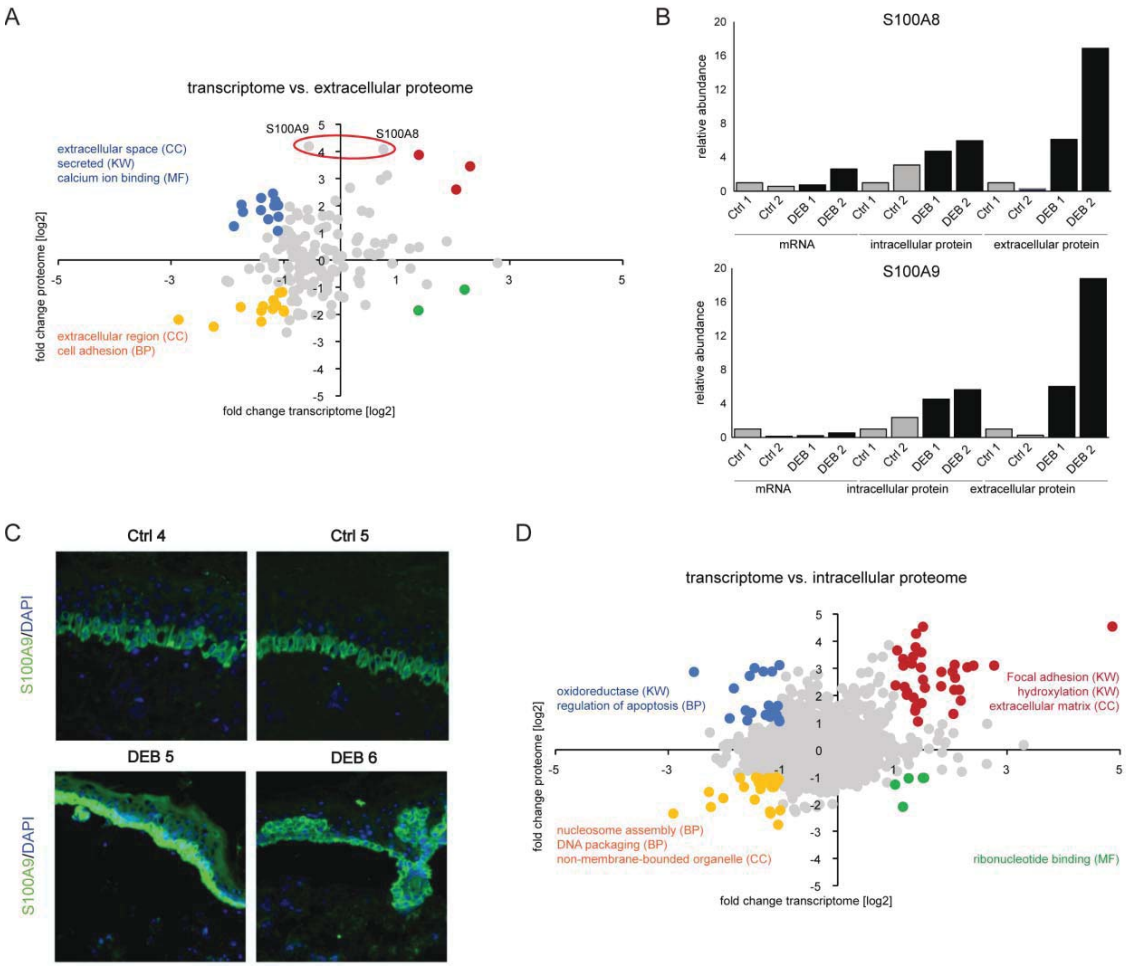

37

Figure 5

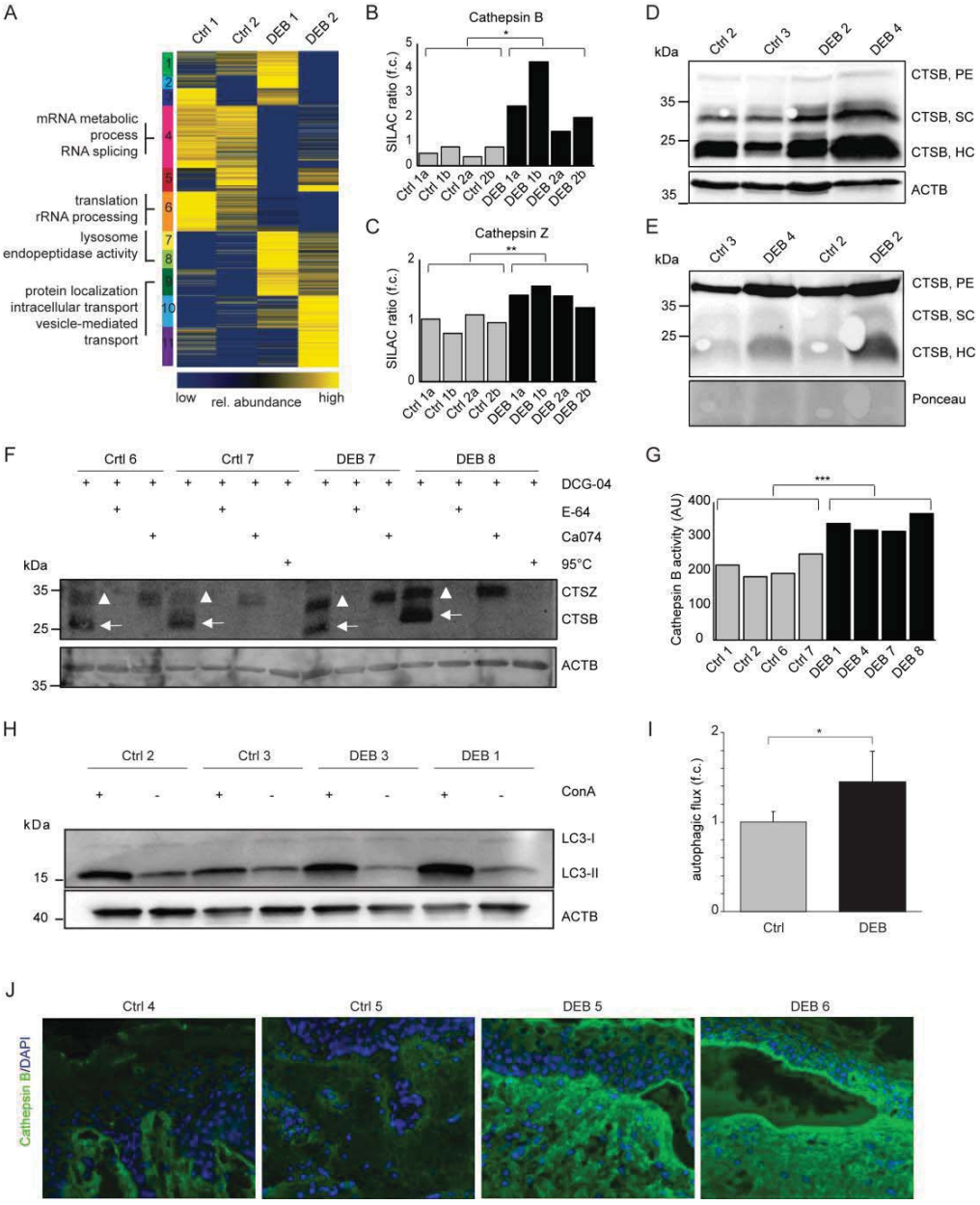

38

Figure 6

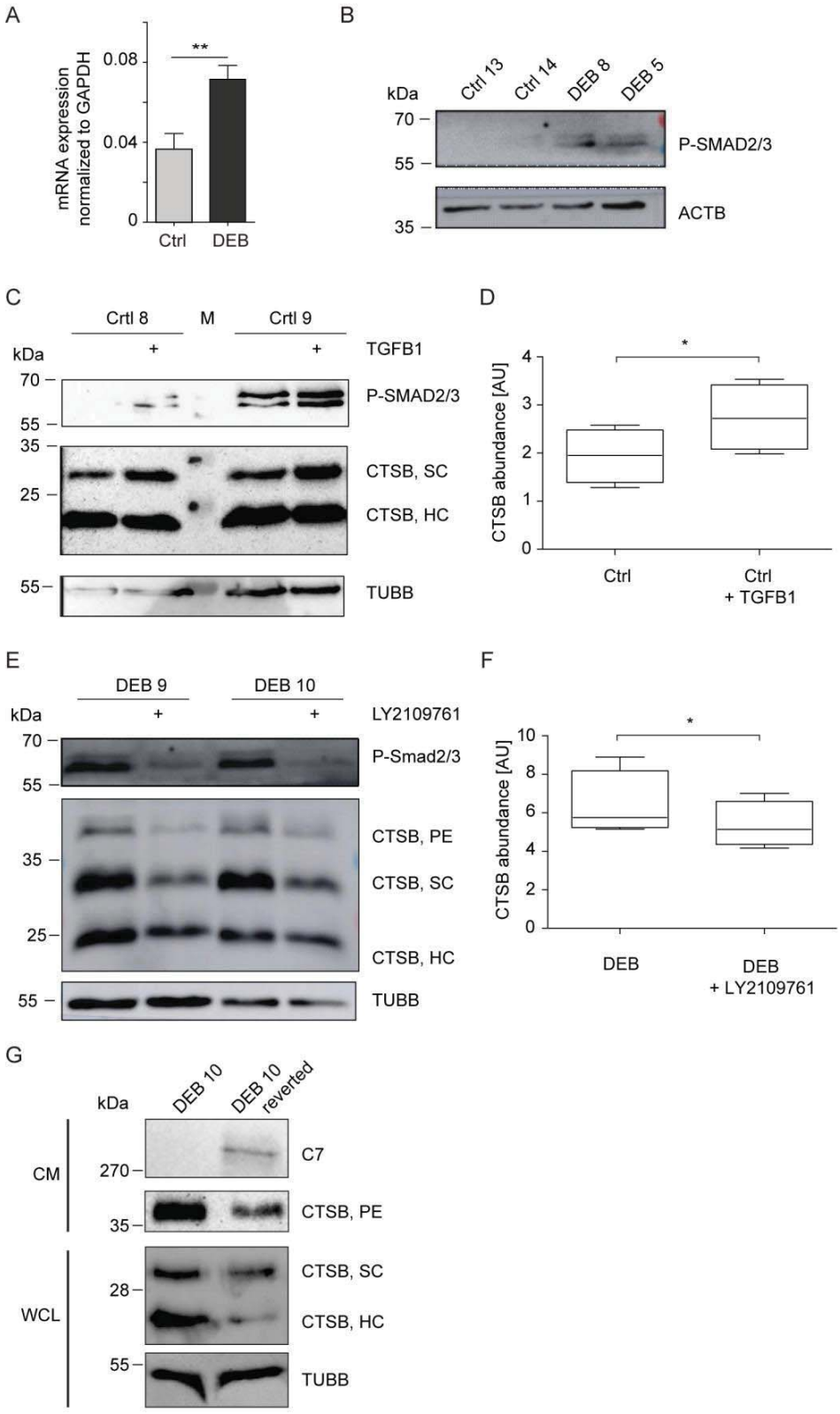

39

Figure 7

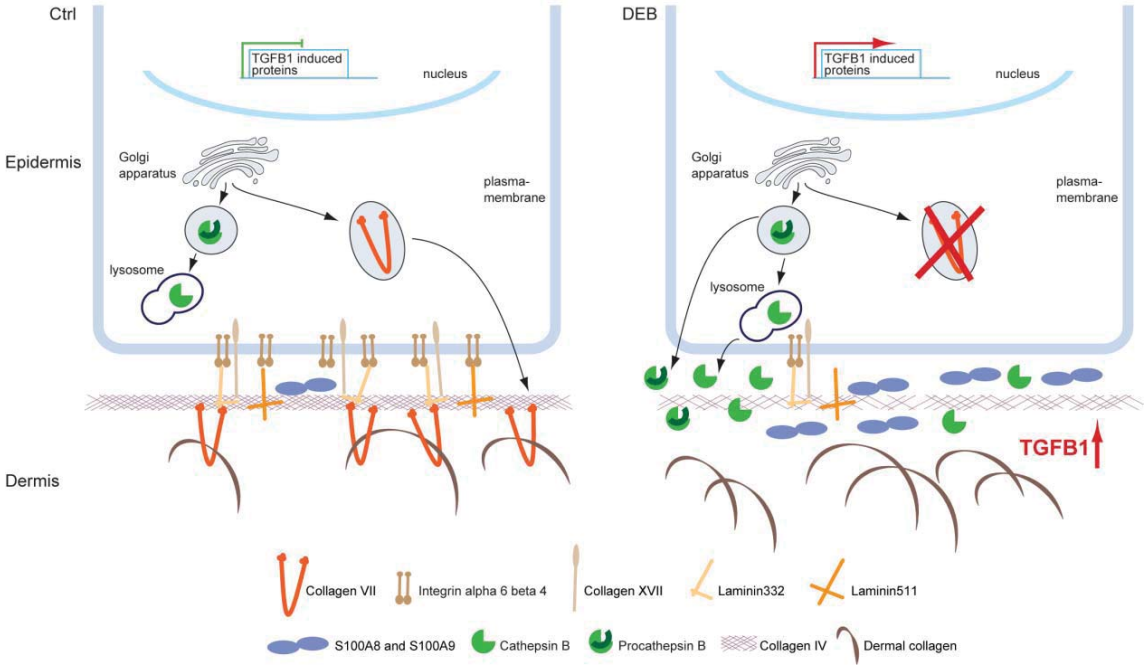

40